Open Research Online

Fluid evolution in CM carbonaceous chondrites tracked through the oxygen isotopic compositions of carbonates

Journal Item

For guidance on citations see FAQs.

Version: Version of Record

oro.open.ac.uk

Fluid evolution in CM carbonaceous chondrites tracked through the oxygen isotopic compositions of carbonates

P. Lindgren [a], M.R. Lee [a,*], N.A. Starkey [b], I.A. Franchi [b]

[a] *School of Geographical and Earth Sciences, Gregory Building, Lilybank Gardens, Glasgow G12 8QQ, United Kingdom*
[b] *Planetary and Space Sciences, The Open University, Milton Keynes MK7 6AA, United Kingdom*

Abstract

The oxygen isotopic compositions of calcite grains in four CM carbonaceous chondrites have been determined by Nano-SIMS, and results reveal that aqueous solutions evolved in a similar manner between parent body regions with different intensities of aqueous alteration. Two types of calcite were identified in Murchison, Mighei, Cold Bokkeveld and LaPaz Icefield 031166 by differences in their petrographic properties and oxygen isotope values. Type 1 calcite occurs as small equant grains that formed by filling of pore spaces in meteorite matrices during the earliest stages of alteration. On average, the type 1 grains have a $\delta^{18}O$ of ∼32–36‰ (VSMOW), and $\Delta^{17}O$ of between ∼2‰ and −1‰. Most grains of type 2 calcite precipitated after type 1. They contain micropores and inclusions, and have replaced ferromagnesian silicate minerals. Type 2 calcite has an average $\delta^{18}O$ of ∼21–24‰ (VSMOW) and a $\Delta^{17}O$ of between ∼−1‰ and −3‰. Such consistent isotopic differences between the two calcite types show that they formed in discrete episodes and from solutions whose $\delta^{18}O$ and $\delta^{17}O$ values had changed by reaction with parent body silicates, as predicted by the closed-system model for aqueous alteration. Temperatures are likely to have increased over the timespan of calcite precipitation, possibly owing to exothermic serpentinisation. The most highly altered CM chondrites commonly contain dolomite in addition to calcite. Dolomite grains in two previously studied CM chondrites have a narrow range in $\delta^{18}O$ (∼25–29‰ VSMOW), with $\Delta^{17}O$ ∼−1‰ to −3‰. These grains are likely to have precipitated between types 1 and 2 calcite, and in response to a transient heating event and/or a brief increase in fluid magnesium/calcium ratios. In spite of this evidence for localised excursions in temperature and/or solution chemistry, the carbonate oxygen isotope record shows that fluid evolution was comparable between many parent body regions. The CM carbonaceous chondrites studied here therefore sample either several parent bodies with a very similar initial composition and evolution or, more probably, a single C-type asteroid.

1. INTRODUCTION

C-type asteroids are rich in water, hydroxyls and organics (Clark et al., 2010), and so are of particular importance for understanding the transfer throughout the Solar System of volatiles and other compounds of biological importance.

In recognition of their significance, these bodies are the targets of forthcoming missions, including OSIRIS-Rex, which will return samples of (101955) Bennu (Emery et al., 2014; Lauretta et al., 2015). Pieces of one or more C-type asteroids are also available for study in the form of Mighei-like (CM) carbonaceous chondrite meteorites (e.g., Burbine et al., 2002; Kasuga et al., 2013). The principal carriers of hydroxyls in these rocks are phyllosilicates, which have formed by the aqueous alteration of primary silicates, metals, sulphides and amorphous materials (e.g., McSween, 1979a,b; Bunch

and Chang, 1980; Tomeoka and Buseck, 1985). The liquid water that mediated alteration originated from melting of ices in the parent body interior (DuFresne and Anders, 1962), but the nature of these fluids and their spatial and temporal dynamics are poorly understood. Currently unanswered questions include: was alteration a single event, or did it take place in multiple pulses? was the water static, or did it flow? were temperatures stable, or did they change over the timespan of aqueous alteration? did all parent body regions evolve in the same manner, or did alteration trajectories locally differ? These questions have been addressed in models of parent body evolution, some of which postulate a closed system (e.g., Clayton and Mayeda, 1984, 1999; Bland et al., 2009; Velbel et al., 2012) whereas others invoke single-pass or convective fluid flow (e.g., Young et al., 1999; Young, 2001; Palguta et al., 2010).

Fresh insights into parent body aqueous alteration may come from carbonates, which host 0.03–0.60 wt.% of the 1.2–3.1 wt.% carbon in CM meteorites (Alexander et al., 2013, 2015). These minerals comprise aragonite, calcite, dolomite and breunnerite (Barber, 1981; Johnson and Prinz, 1993; Lee, 1993; Lee and Ellen, 2008; de Leuw et al., 2010; Lee et al., 2014). ^{53}Mn-^{53}Cr dating has shown that calcite and dolomite precipitated within five million years of Solar System formation (Fujiya et al., 2012). The carbon and oxygen isotopic compositions of these carbonate minerals can be used to explore the provenance of aqueous solutions and the nature of their interaction with the parent body. Previous studies have shown that individual CM chondrites contain populations of carbonate minerals whose oxygen isotopic compositions provide good evidence for multiple episodes of precipitation from aqueous fluids of different oxygen isotopic compositions and/or temperatures (e.g., Benedix et al., 2003; Guo and Eiler, 2007; Tyra et al., 2012, 2016; Lee et al., 2013; Fujiya et al., 2015).

Here we have determined the oxygen isotopic compositions of calcite grains in four CM carbonaceous chondrites in order to investigate how aqueous alteration environments evolved within and between different parent body regions. As the selected meteorites have been altered to contrasting extents, their aqueous systems are likely to have varied in one or more of: (i) temperature; (ii) longevity; (iii) water/rock ratio. If, for example, results indicate that carbonates in the different meteorites formed at contrasting temperatures, then the implications could be that the CM chondrites have sampled different parts of an aqueous system containing water moving along a thermal gradient. Conversely, strong similarities in fluid evolution between meteorites may be more indicative of a static aqueous system within parent body regions that were originally chemically and isotopically homogeneous. Either way, results of this work will provide new insights into the nature of one of the earliest Solar System processes.

2. MATERIALS AND METHODS

2.1. Petrographic characterisation of carbonates

This study has used the CM carbonaceous chondrites Murchison, Mighei, Cold Bokkeveld and LaPaz Icefield (LAP) 031166. These meteorites differ in their degree of aqueous alteration, as expressed using three classification schemes (Table 1). Hereafter we refer to the extent of aqueous alteration of the CM chondrites using the petrologic subtype notation of Rubin et al. (2007).

One carbon coated thin section or polished block of each of the meteorites was studied (Table 1). Calcite grains were located and characterised by backscattered electron (BSE) and secondary electron (SE) imaging using two field-emission scanning electron microscopes (SEM), both operated at high vacuum and 20 kV/$\sim$2 nA: a FEI Quanta 200F and a Zeiss Sigma. Chemical analyses and elemental maps were acquired by energy-dispersive X-ray spectroscopy (EDS) using an Oxford AZtec microanalysis system attached to the Zeiss SEM. The abundances of calcite grains were determined by point counting on the Quanta SEM, whereby the sample was manually systematically traversed (using the frame-by-frame stage movement function), and the material in the centre of the field of view at each step was identified by imaging and EDS. The point counting was undertaken at $\times$2000 magnification and a step-size of 150 μm, with 3000 points typically being counted for each meteorite.

2.2. NanoSIMS oxygen isotope analyses of carbonates

Owing to the small size of the calcite grains they were analysed for their oxygen isotope composition using a Nano Secondary Ion Mass Spectrometry (SIMS) 50L at the Open University (OU), U.K. (Figs. S1–S4). The analyses were performed by rastering the focussed primary beam over a small area and integrating the total ion signal. A Cs^+ ion beam with a current of $\sim$30 pA was used for the analyses ($\sim$60 pA for pre-sputter). Secondary ions were measured in multi-collection mode, with ^{16}O measured on a Faraday cup, and ^{17}O, ^{18}O, $^{24}Mg^{16}O$, $^{40}Ca^{16}O$ and $^{56}Fe^{16}O$ measured on electron multipliers. The major cation oxides allowed real time monitoring of the mineral compositions. The mass resolving power was set to $>$10,000 (Cameca, NanoSIMS definition, based on the measured peak width it is the slope between 10% and 90% of the peak), which was sufficient to resolve the interference of ^{16}OH on the ^{17}O peak. Charge compensation was applied using the electron gun. Areas for analysis were 5×5 μm or 3×3 μm, with a larger area for pre-sputter (7×7 μm) in order to implant Cs ions evenly and reach sputter equilibrium across the area to be analysed. Analysis times, including pre-sputter, were typically $\sim$8 min with total counts of ^{16}O in a single analysis being 6×10^9. Isotope ratios were normalised to Vienna Standard Mean Ocean Water (VSMOW) using analyses of a calcite standard that bracketed the sample analyses in order to generate $\delta^{17}O$ and $\delta^{18}O$ values, and also to provide corrections for instrumental mass fractionation. The errors quoted combine internal errors for each analysis with the standard deviation of the mean of the associated standards.

Calcite analyses used an in-house calcite standard with a composition of $\delta^{18}O$ 15.47 ± 0.07‰ (1σ) VSMOW that was determined from six replicate analyses on a ThermoGasbench II connected to a Delta Advantage mass spectrome-

Table 1
The CM carbonaceous chondrite meteorites studied and their degree of aqueous alteration.

Meteorite	Sample number (type)	Recovery	Aqueous alteration indices		
			Petrologic[3]	fP[4]	Water/OH[5]
Murchison	BM1988.M23, P19260 (PB)[1]	Fall, 1969, Australia	CM2.5	1.5	1.6
Mighei	P725310 (PTS)[1]	Fall, 1889, Ukraine	CM2.3	1.4	1.6
Cold Bokkeveld	BM 1727, P1925610 (PB)[1]	Fall, 1838, South Africa	CM2.2	1.4	1.3
LAP 031166	15 (PTS)[2]	Find, 2003, Antarctica	CM2.1	na	na

PB = Polished resin block.
PTS = Polished thin section.
na denotes not analysed.
[1] Loaned by the Natural History Museum London.
[2] Loaned by the NASA Johnson Space Center Antarctic meteorite collection.
[3] The petrologic subtype scheme (Rubin et al., 2007).
[4] Classification based on the normalised fraction of phyllosilicate (Howard et al., 2015).
[5] Classification based on bulk water/OH content (Alexander et al., 2013).

ter. For these measurements powdered aliquots were reacted with anhydrous H_3PO_4 at $72 \pm 0.1\ °C$ for 1 h. The CO_2 generated was then flushed from the head-space of the reaction vessel, dried through Nafian traps before being passed through a Poraplot Q fused silica capillary column to separate other possible contaminants prior to analyses on the mass spectrometer. For the standards, $\delta^{17}O$ was assumed to lie on the terrestrial fractionation line (TFL; defined as $\delta^{17}O = 0.52 \times \delta^{18}O$). Ten analyses of the calcite standard gave a reproducibility of ± 1.2–1.4‰ (2σ) for $\delta^{18}O$, and ± 1.2–2.1‰ (2σ) for $\Delta^{17}O$. The sample and standard were positioned in separate blocks mounted on the same sample holder. Using identical analytical procedures to those presented here, Starkey and Franchi (2013) found no statistically significant variation in oxygen isotope ratios when measuring polished samples of San Carlos olivine mounted in different positions across the NanoSIMS holder (up to 40 mm distance apart). NanoSIMS results are expressed as $\delta^{17}O$, $\delta^{18}O$ and $\Delta^{17}O$ (i.e. $\delta^{17}O$–$0.52 \times \delta^{18}O$), where $\Delta^{17}O$ is a measure of departure from the TFL.

3. RESULTS

3.1. Calcite abundance and petrographic characteristics

Calcite in the four CM chondrites ranges in abundance from 1.23 to 1.87 vol.% (Table 2). Two petrographically distinct types of grains can be recognised in each meteorite, and are referred to as types 1 and 2 (after Tyra et al., 2012) (Fig. 1). Type 1 grains occur in the fine-grained matrix

Table 2
Abundance (vol.%) of the two calcite types as quantified by SEM point counting.

Meteorite	Type 1	Type 2	Type 1/Type 2 ratio
Murchison	1.50	0.30	5.0
Mighei	1.70	0.10	17.0
Cold Bokkeveld	1.37	0.50	2.7
LAP 031166	0.63	0.60	1.1

(Fig. 1a and b). They are typically equant and monocrystalline, can have euhedral terminations, and are rimmed by serpentine and/or tochilinite. Type 2 grains may be present in the matrix but are more commonly hosted in chondrules or chondrule pseudomorphs (Fig. 1c and d). These grains are usually larger than type 1 (some grains can be several hundreds of micrometres in size; Lee et al., 2014), lack a characteristic shape, are typically polycrystalline, contain micropores and inclusions, and lack serpentine/-tochilinite rims (Fig. 1c–f). Type 1 calcite is more abundant than type 2 in each meteorite (Table 2).

3.2. Oxygen isotopic composition of calcite

Calcite grains in each of the four studied meteorites can differ significantly in their oxygen isotopic compositions. The NanoSIMS results are here described with reference to the two petrographic types of calcite (Table 3, Fig. 2 and 3, Figs. S1–S4). The five grains of type 1 calcite in Murchison are distinct in their $\delta^{18}O$ values from the three type 2 grains ($\sim$34–30‰ vs 26–18‰, respectively). One of the type 1 analyses plots below the TFL, as do all of the type 2 datapoints. Previous NanoSIMS studies of Murchison calcite have recorded high $\delta^{18}O$ values that are consistent with mainly analysing type 1 grains: 27–37‰ (Brearley et al., 1999), 34–38‰ (Bonal et al., 2010), 30–39‰ (Horstmann et al., 2014), 33–34‰ (Fujiya et al., 2015). Mighei type 1 grains have a wide range in $\delta^{18}O$ ($\sim$16–40‰), and all but one is within error of the TFL. The sole type 2 grain analysed has a $\delta^{18}O$ value in the middle of the type 1 group and plots on the TFL. Nine type 1 grains were analysed in Cold Bokkeveld, and have a $\delta^{18}O$ of 30–39‰. The four type 2 grains have a broader compositional range ($\delta^{18}O$ 12–37‰). Five Cold Bokkeveld grains plot below the TFL (three type 1, two type 2) whereas the other eight are within error of the line. The LAP 031166 data form two clusters. The five type 1 grains have a $\delta^{18}O$ of $\sim$35–39‰. Three of the four type 2 grains are much lighter ($\delta^{18}O$ 17–22‰) whereas the other plots within the type 1 cluster. Two of the type 1 grains are above the TFL and one of the type 2 grains is below the TFL. Tyra
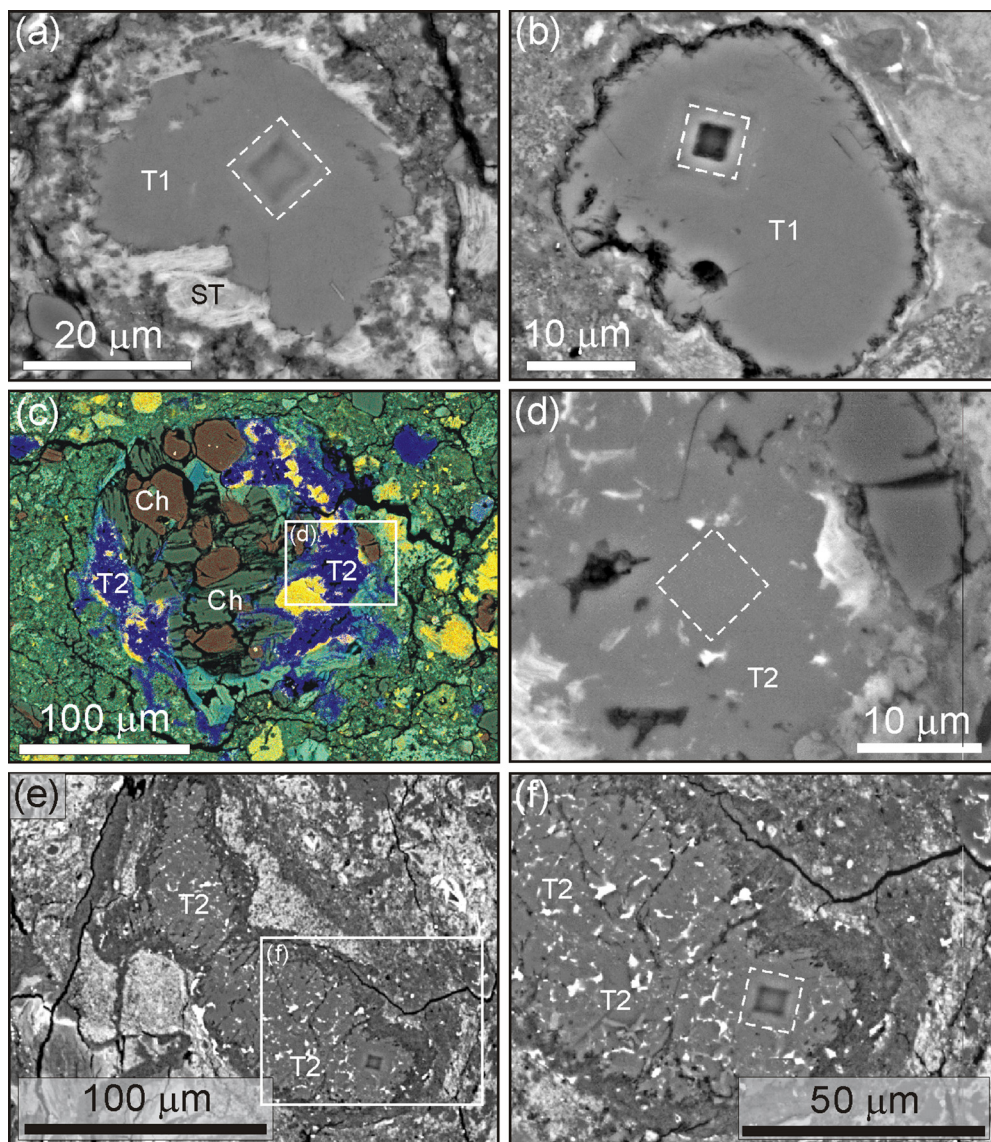
Fig. 1. Images of type 1 (T1) and type 2 (T2) calcite grains that were analysed by NanoSIMS, with the datapoints identified (all analysed grains are shown in Figs. S1–S4). (a) BSE image of a type 1 grain in Mighei (Mig_cct1_7). The serpentine/tochilinite grain rim is white, and labelled ST. (b) BSE image of a type 1 grain in Cold Bokkeveld (CB_cct1_14). (c) Type 2 calcite in Mighei, which has partially replaced a chondrule. The image is made from a false-coloured X-ray map that has been overlain on a SE image. The X-ray map has been made by blending colours from four element maps: Mg (red), Si (turquoise), S (yellow) and Ca (blue). This blending renders the chondrule silicates (Ch) dark green and brown, sulphides yellow, and calcite blue. (d) BSE image of the boxed area in (c) showing the location of point Mig_cct2_1. (e) BSE image of type 2 calcite in LAP 031166. (f) BSE image of the boxed area in (e) showing location of point LAP_cct2_1. (For interpretation of the references to colour in this figure legend, the reader is referred to the web version of this article.)

et al. (2007, 2012) found that types 1 and 2 calcite in the EET 96006-paired meteorites were chemically indistinguishable, thus showing that the trace element composition of pore fluids had not changed in parallel with their oxygen isotopic composition (or temperature).

4. DISCUSSION

Calcite grains differ in their oxygen isotopic compositions within and between each of the four studied CM chondrites, thus showing that these meteorites contain a temporally and/or spatially resolved record of parent body evolution. In order to maximise the new insights that can be gained from the isotope data, they are discussed below in the framework of the petrographic properties and contexts of the calcite grains, and synthesised with results from previous grain-scale and bulk isotopic studies. These results will then enable testing of models for the evolution of aqueous solutions in C-type asteroids within the first five million years of Solar System history.

Table 3
Oxygen isotope compositions of calcite grains obtained by NanoSIMS.

Meteorite	Grain type	$\delta^{17}O$ (‰)	2σ	$\delta^{18}O$ (‰)	2σ	$\Delta^{17}O$ (‰)	2σ
Murchison							
Murch_cct1_3	Type 1 calcite	18.3	1.2	34.1	0.8	0.5	1.3
Murch_cct1_4	Type 1 calcite	14.9	1.2	30.8	0.8	−1.1	1.3
Murch_cct1_5	Type 1 calcite	18.1	1.2	33.6	0.8	0.7	1.3
Murch_cct1_7	Type 1 calcite	16.8	1.2	33.3	0.8	−0.5	1.3
Murch_cct1_8	Type 1 calcite	12.9	1.2	30.1	0.8	−2.8	1.3
Murch_cct2_1[a]	Type 2 calcite	6.3	1.4	20.3	1.2	−4.3	1.6
Murch_cct2_1[c]	Type 2 calcite	7.8	1.4	18.5	1.2	−1.8	1.7
Murch_cct2_2	Type 2 calcite	7.1	1.4	19.2	1.2	−2.9	1.6
Murch_cct2_3	Type 2 calcite	11.4	1.4	26.3	1.2	−2.3	1.6
Mighei							
Mig_cct1_1	Type 1 calcite	13.7	2.1	26.4	1.1	0.0	2.2
Mig_cct1_4[a]	Type 1 calcite	9.1	2.0	17.5	1.1	0.0	2.2
Mig_cct1_4[b]	Type 1 calcite	5.3	2.0	16.4	1.0	−3.2	2.1
Mig_cct1_4[c]	Type 1 calcite	7.9	2.0	17.8	1.0	−1.3	2.1
Mig_cct1_6	Type 1 calcite	19.3	2.0	35.8	1.0	0.7	2.1
Mig_cct1_7	Type 1 calcite	18.5	2.0	35.2	1.0	0.2	2.2
Mig_cct1_18	Type 1 calcite	21.7	2.2	38.3	1.2	1.8	2.3
Mig_cct1_19	Type 1 calcite	22.3	2.2	40.0	1.2	1.5	2.4
Mig_cct2_1	Type 2 calcite	11.7	2.2	25.9	1.2	−1.7	2.4
Cold Bokkeveld							
CB_cct1_3	Type 1 calcite	12.1	2.3	31.9	1.6	−4.5	2.6
CB_cct1_6	Type 1 calcite	17.0	2.2	34.6	1.6	−1.0	2.5
CB_cct1_8	Type 1 calcite	17.5	2.5	37.5	0.9	−1.9	2.6
CB_cct1_12	Type 1 calcite	12.1	2.5	30.8	0.9	−3.9	2.6
CB_cct1_14	Type 1 calcite	15.8	2.0	35.4	1.2	−2.6	2.2
CB_cct1_18_5	Type 1 calcite	21.0	1.9	37.2	1.7	1.7	2.2
CB_cct1_18_6	Type 1 calcite	18.1	1.9	35.1	1.7	−0.2	2.2
CB_cct1_19	Type 1 calcite	20.6	1.9	38.8	1.7	0.5	2.2
CB_cct1_20	Type 1 calcite	18.9	2.3	36.2	1.6	0.1	2.6
CB_cct2_2	Type 2 calcite	2.5	2.3	11.9	1.6	−3.7	2.5
CB_cct2_4	Type 2 calcite	16.9	2.3	36.8	1.2	−2.2	2.5
CB_cct2_6	Type 2 calcite	11.8	1.9	27.0	0.8	−2.2	2.0
CB_cct2_7	Type 2 calcite	7.8	2.0	18.6	1.3	−1.8	2.2
LAP 031166							
LAP_cct1_5	Type 1 calcite	21.5	2.1	36.3	1.1	2.6	2.3
LAP_cct1_7	Type 1 calcite	19.9	2.0	37.1	1.1	0.6	2.1
LAP_cct1_8	Type 1 calcite	19.6	1.9	34.5	1.1	1.6	2.1
LAP_cct1_9	Type 1 calcite	20.2	1.9	34.6	1.0	2.3	2.0
LAP_cct1_10	Type 1 calcite	21.0	1.9	39.3	1.0	0.6	2.1
LAP_cct2_1	Type 2 calcite	9.0	2.0	22.2	1.1	−2.5	2.2
LAP_cct2_2[a]	Type 2 calcite	8.3	2.1	20.5	1.1	−2.3	2.3
LAP_cct2_2[b]	Type 2 calcite	10.4	2.2	20.6	1.1	−0.3	2.3
LAP_cct2_2[c]	Type 2 calcite	7.4	2.1	18.0	1.1	−1.9	2.3
LAP_cct2_3	Type 2 calcite	8.1	2.1	17.0	1.1	−0.8	2.3
LAP_cct2	Type 2 calcite	18.5	2.1	35.9	1.1	−0.2	2.3

Isotope values are expressed relative to VSMOW.
Superscripts [a], [b], [c] denote multiple analyses of the same grain.
An image of each analysed grain is provided in Figs. S1–S4.

4.1. Formation of types 1 and 2 calcite

The petrographic characteristics of types 1 and 2 calcite grains, and the petrologic subtypes of meteorites within which they occur, can help to constrain when these carbonates formed during aqueous alteration. This information can then be used to 'pin' the oxygen isotope data obtained by NanoSIMS to specific periods in parent body evolution.

Given that most grains of type 1 calcite have been partially replaced by serpentine and/or tochilinite, whereas none of the type 2 grains have been so affected, type 1 calcite is interpreted to have formed first. The euhedral shapes of some of the type 1 grains and their lack of inclusions suggest that they have filled pore spaces in the matrix, possibly after ice grains (as discussed by Lee et al., 2014). The presence of type 1 calcite in Murchison shows that it had
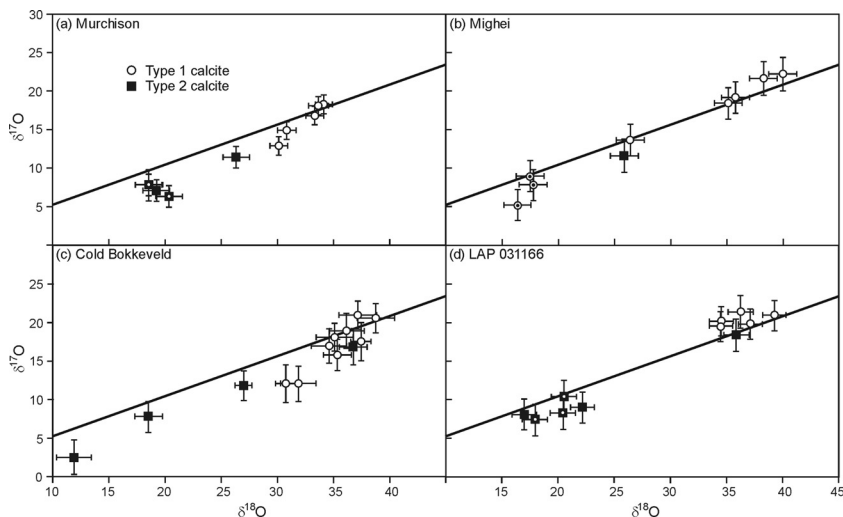
Fig. 2. Three-isotope plots of the oxygen isotopic compositions of calcite in: (a) Murchison, (b) Mighei, (c) Cold Bokkeveld and (d) LAP 031166. Those datapoints containing a central dot are from the same grain, and the solid line in each plot is the TFL. The data are listed in Table 2, and images of each analysed grain are in Figs. S1–S4.
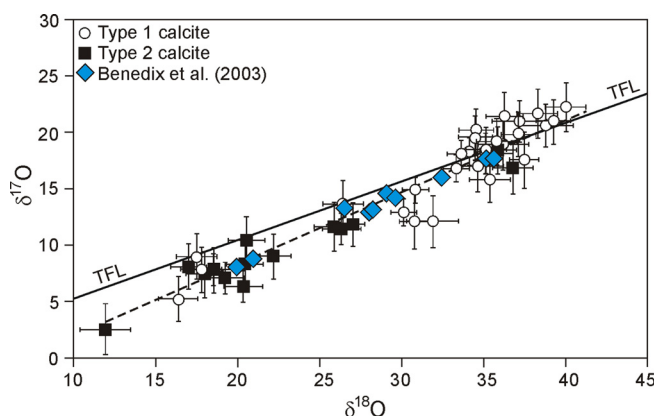

Fig. 3. Three-isotope plot with the 42 oxygen isotope analyses obtained in the present study. The dashed black regression line plotted through these points has the equation $\delta^{17}O = 0.67(\pm 0.06) \times \delta^{18}O - 5.3(\pm 1.8)$ (2σ; MSWD = 2.1). The solid black line is the TFL. Blue coloured diamonds denote bulk analyses of carbonates (25° acidification) in Murchison, Murray, Mighei, Nogoya and Cold Bokkeveld by Benedix et al. (2003). The regression line for these 11 points is not shown, but has an equation of $\delta^{17}O = 0.62(\pm 0.04) \times \delta^{18}O - 4.1(\pm 1.1)$ (2σ; MSWD = 1.7). (For interpretation of the references to colour in this figure legend, the reader is referred to the web version of this article.)

formed by the time that aqueous alteration had reached the CM2.5 stage. As calcite with similar petrographic characteristics also occurs in Elephant Morraine (EET) 96029 and Paris, which are the least aqueously altered CM chondrites yet described (both CM2.7) (Hewins et al., 2014; Marrocchi et al., 2014; Lee et al., 2016), type 1 calcite must have been one of the first products of parent body aqueous alteration. The calcium required to produce calcite at this early stage is most likely to have been sourced from the dissolution of chondrule mesostasis, plagioclase and melilite. These components are so susceptible to aqueous alteration that they are very scarce even in EET 96029 and Paris (Marrocchi et al., 2014; Rubin, 2015; Lee et al., 2016). Thus, a significant proportion of the type 1 calcite grains in each of the four meteorites is interpreted to have formed by the time that they had been aqueously altered to a level

equivalent to CM2.7 2.5. The occurrence of type 1 calcite in LAP 031166 (CM2.1) shows that these early-formed carbonate grains were preserved during subsequent aqueous processing. The serpentine and tochilinite that replaced type 1 calcite is likely to have formed from ions derived from components that were less susceptible to dissolution, including olivine, Fe-sulphide and Fe, Ni metal.

The common presence of type 2 calcite within chondrules, occasionally forming hundreds of micrometre sized pseudomorphs (Lee et al., 2014), indicates that it is a replacement product of primary ferromagnesian silicates. As type 2 calcite occurs in Murchison, it can have precipitated before aqueous alteration had progressed beyond CM2.5; formation even earlier is suggested by the presence of grains with comparable petrographic properties in EET 96029 (Lee et al., 2014, 2016). Another line of evidence

for a relatively early origin of some of the type 2 calcite is that the chondrule-hosted silicate minerals that it has replaced are progressively destroyed during aqueous alteration; they are scarce in CM2.1 meteorites and absent from CM2.0s (Rubin et al., 2007). Thus, the type 2 calcite that occurs in the most highly altered CM chondrites (i.e., LAP 031166) must have precipitated whilst they still contained significant amounts of primary ferromagnesian silicates, and so before they had reached a level of aqueous alteration equivalent to ∼CM2.1. The source of Ca for type 2 calcite is difficult to determine. It could have been derived from the dissolution of pyroxene or type 1 calcite, although input of Ca from other parent body regions is possible, and would be consistent with the presence of a vein of type 2 calcite in the CM carbonaceous chondrite Lonewolf Nunataks (LON) 94101 (Lindgren et al., 2011; Lee et al., 2013).

The occurrence of types 1 and 2 calcite in mildly altered meteorites such as Murchison shows that these carbonate grains formed mainly in the early stages of parent body processing. Such a timing is consistent with the poor correlation between the abundance of calcite in the CM chondrites and their degree of aqueous alteration (Lee et al., 2014; Alexander et al., 2015). Only if calcite had precipitated throughout aqueous alteration would its abundance be expected to correlate closely to petrologic subtype.

4.2. Determinants of carbonate oxygen isotopic compositions

Having identified the approximate points at which calcite grains formed during aqueous alteration (i.e., much of the type 1 before CM2.7 2.5; type 2 between ∼CM2.7 2.5 and ∼CM2.1), their oxygen isotopic compositions can be interpreted in the context of parent body evolution. The following discussions assume that carbonate mineral grains preserve a 'snapshot' of the oxygen isotopic compositions of solutions from which they originally precipitated (i.e., they have not re-equilibrated in step with changing fluid properties; Tyra et al., 2012).

The range in oxygen isotope values obtained from carbonate grains within any one meteorite is interpreted to reflect changes over time in the oxygen isotopic compositions and/or temperatures of aqueous solutions. The relative importance of fluid composition and temperature can be assessed by asking how $\delta^{18}O$, $\delta^{17}O$ and $\Delta^{17}O$ vary between grains. For example, if a population of grains had precipitated from a fluid of invariant $\Delta^{17}O$ and changing temperature, $\delta^{18}O$ and $\delta^{17}O$ values would covary to form an array with a slope of 0.52 in a three-isotope plot (i.e., mass-dependent fractionation, parallel to the TFL). Those grains that formed at a higher temperature would have a lower $\delta^{18}O$ and $\delta^{17}O$. Conversely, calcite grains that had precipitated from a fluid that was initially ^{16}O-poor but had exchanged with a component that had a negative $\Delta^{17}O$, by interaction with parent body silicates at a constant temperature, would form an array with a slope that is steeper than 0.52. A regression line plotted through the 42 analyses of calcite obtained in the present study (Fig. 3) has an equation of $\delta^{17}O = 0.67(\pm0.06) \times \delta^{18}O$ $-5.3(\pm1.8)$ (2σ; MSWD = 2.1), thus demonstrating a change in the oxygen isotopic compositions of the fluids (although this finding

does not discount a simultaneous change in temperature). The equation of a line regressed through 81 analyses of calcite from the CM chondrites Banten, Cold Bokkeveld, Maribo, Murchison and Nogoya is very similar: $\delta^{17}O = 0.65$ $(\pm0.03) \times \delta^{18}O$ $-5.4(\pm0.9)$ (2σ; MSWD = 1.3) (Horstmann et al., 2014). Whilst there is clear evidence for a change in fluid composition, some of the data in Fig. 3 could suggest that temperatures changed when $\Delta^{17}O$ was static. Specifically, a line of slope 0.52 could be fitted to those grains with a $\delta^{18}O$ of less than ∼35‰.

There is good evidence for correlated changes to $\delta^{18}O$ and $\Delta^{17}O$ when grains from several CM chondrites are considered together, but this approach may mask differences between meteorites. Therefore, analyses of calcite in the four samples used in the present study are here discussed individually. Murchison and Cold Bokkeveld both show a correlated fall in $\delta^{18}O$ and $\Delta^{17}O$ (Table 3, Fig. 2). With regards to Murchison, the four analyses with the highest $\delta^{18}O$ are within error of the TFL, whereas the five analyses with a lower $\delta^{18}O$ have negative $\Delta^{17}O$. Eight of the Cold Bokkeveld analyses plot in a cluster ($\delta^{18}O$ ∼35 39‰) and all but one of them is within error of the TFL. Four of the five analyses with a lower $\delta^{18}O$ are below the TFL. The Mighei data show less of a clear trend; only one data-point is below the TFL, although it is the analysis with the lowest $\delta^{18}O$. The LAP 031166 grains do not show a consistent relationship between $\delta^{18}O$ and $\Delta^{17}O$. Eight of the 11 analyses are within error of the TFL; the two that plot above the TFL are within the high $\delta^{18}O$ cluster, and the one that is below the TFL is in the low $\delta^{18}O$ cluster. Therefore, the populations of grains in individual meteorites also show that $\delta^{18}O$ and $\Delta^{17}O$ covary, indicating a change in the oxygen isotopic composition of the solutions, although the evidence is strongest in Murchison and Cold Bokkeveld. This result is consistent with slopes of 0.61 0.62 obtained for regression lines plotted through analyses of calcite grains in each of Sutter's Mill, EET 96006-paired and LON 94101 (Jenniskens et al., 2012; Tyra et al., 2012; Lee et al., 2013).

4.3. Relative timescales of fluid evolution

NanoSIMS data from grains in individual CM chondrites and in multiple meteorites demonstrate a temporal change in the oxygen isotopic composition of aqueous solutions, but do not reveal the 'direction' of evolution. As the studied meteorites contain two generations of calcite, any consistent differences between them will reveal how the fluids evolved. Types 1 and 2 calcite differ in their average $\delta^{18}O$ values in Murchison, Cold Bokkeveld and LAP 031166, and also in three other CM chondrites studied previously (Table 4). As the average $\delta^{18}O$ value of type 1 calcite in all of these meteorites is heavier than type 2, solutions must have evolved towards lower values of $\delta^{18}O$ and $\Delta^{17}O$ in each of these six parent body regions. Although the average $\delta^{18}O$ values of types 1 and 2 calcite are quite different in Murchison, Cold Bokkeveld and LAP 031166 (Table 4), in two of these meteorites some type 2 grains plot in the type 1 field (Fig. 2a and b). These apparent anomalies may be because: (i) the grains in question

Table 4
Average oxygen isotopic compositions of types 1 and 2 calcite in six meteorites, including three analysed in the present study.

	$\delta^{18}O$	$\Delta^{17}O$	$\delta^{18}O$	$\Delta^{17}O$
	Type 1 calcite		Type 2 calcite	
Murchison	$32.4 \pm 1.8‰$ (1σ)	$-0.6 \pm 1.4‰$ (1σ)	$21.1 \pm 3.6‰$ (1σ)	$-2.8 \pm 1.1‰$ (1σ)
Cold Bokkeveld	$35.3 \pm 2.6‰$ (1σ)	$-1.3 \pm 2.1‰$ (1σ)	$23.6 \pm 10.8‰$ (1σ)	$-2.5 \pm 0.8‰$ (1σ)
LAP 031166	$36.4 \pm 2.0‰$ (1σ)	$1.5 \pm 0.9‰$ (1σ)	$22.4 \pm 6.9‰$ (1σ)	$-1.3 \pm 1.0‰$ (1σ)
EET 96006, 16, 17, 19[1]	$33.7 \pm 2.3‰$ (1σ)	$-0.81 \pm 0.90‰$ (1σ)	$19.4 \pm 1.5‰$ (1σ)	$-1.98 \pm 0.90‰$ (1σ)
LON 94101[2]	$37.5 \pm 0.7‰$ (1σ)	$1.4 \pm 1.1‰$ (1σ)	$18.4 \pm 0.3‰$ (1σ)	$-0.50 \pm 0.50‰$ (1σ)
Nogoya[3]	$34.7‰$	$-2.5‰$	$19.3‰$	$-5.4‰$

Mighei is not included in this table as only one analysis of a type 2 grain was obtained.
[1] Tyra et al. (2012).
[2] Lee et al. (2013).
[3] Fujiya et al. (2016). Errors not given.

occur in clasts that have a different fluid evolution to the rest of the meteorite; (ii) they are type 1 grains that have been misidentified as type 2; (iii) the two modes of formation of calcite, namely pore filling type 1 and replacive type 2, were not in all cases temporally distinct.

Average isotopic compositions of the two types of calcite are similar in all of the six CM chondrites included in Table 4 (i.e., type 1 $\delta^{18}O$ ~32–38‰; type 2 $\delta^{18}O$ ~18–24‰). Thus, the types 1 and 2 calcite are interpreted to have formed in two episodes, and when aqueous solutions in six parent body regions had reached approximately the same two points in their compositional evolution. Results from Mighei do not fit this pattern. The range in $\delta^{18}O$ of type 1 calcite (16–40‰) suggests that its precipitation was more continuous in the parent body region that this meteorite has sampled.

4.4. Origin and significance of dolomite

Differences in average $\delta^{18}O$ values between grains of types 1 and 2 calcite show that they precipitated at two different points during parent body evolution. In the intervening period aqueous solutions had evolved isotopically by interaction with ^{16}O-rich parent body silicates; temperatures may also have increased. The nature of parent body environments may be explored further using the oxygen isotopic composition of dolomite in two highly aqueously altered CM chondrites: Allan Hills (ALH) 84049 (CM2.0; Tyra et al., 2016) and Sutter's Mill (CM2.0–2.1; Jenniskens et al., 2012) (Table 5).

On the assumption that aqueous solutions in ALH 84049 and Sutter's Mill evolved by a coupled fall in $\delta^{18}O$ and $\Delta^{17}O$ (i.e., in the same manner as revealed by calcite in the six CM chondrites listed in Table 4), the average

Table 5
Average isotopic compositions of dolomite grains in two CM chondrites.

Meteorite	$\delta^{18}O$	$\Delta^{17}O$	n
Sutter's Mill[1]	$24.7 \pm 0.7‰$ (1σ)	$-3.2 \pm 0.4‰$ (1σ)	11
ALH 84049[2]	$28.6 \pm 2.1‰$ (1σ)	$-1.2 \pm 1.3‰$ (1σ)	11

Values expressed relative to VSMOW.
n denotes number of analyses.
[1] Jenniskens et al. (2012).
[2] Tyra et al. (2016).

$\delta^{18}O$ values of dolomite grains in these two meteorites (~25–29‰; Table 5) suggest that they formed between types 1 and 2 calcite. Although types 1 and 2 calcite were not distinguished by Jenniskens et al. (2012), the compositional range of calcite in this CM chondrite is wider than that of dolomite (i.e., $\delta^{18}O$ 13.2–39.2‰ for calcite vs 23.5–26.1‰ for dolomite). Such a difference would be consistent with dolomite forming between separate generations of calcite. Note that contrasts in calcite-water and dolomite-water fractionation factors are insufficient to account for the observed differences in $\delta^{18}O$ values between two minerals (e.g., dolomite precipitated over the 80–350 °C temperature range is enriched in ^{18}O by 0.7–2.6‰ relative to calcite (Horita, 2014)).

As dolomite occurs only in CM2.0–2.2 meteorites (de Leuw et al., 2010; Lee et al., 2014), conditions were conducive to its precipitation just in those parent body regions that were highly aqueously altered. In these regions, the evolving fluids may have briefly surpassed the threshold for dolomite precipitation, for example, owing to a high Mg/Ca ratio. Alternatively, a short-lived increase in temperature could have catalysed dolomite formation by overcoming the barrier to precipitation from the hydration of magnesium ions. The return to calcite precipitation, to form type 2 grains, may have been due to a fall in temperature or a change in fluid chemistry, for example selective removal of magnesium by precipitation of dolomite or Mg-rich serpentine. This model of carbonate precipitation is consistent with the observation that dolomite in the CM chondrites has commonly been replaced by calcite (Lee et al., 2012, 2014), and findings of Tyra et al. (2016) that in ALH 84049 the two carbonate minerals formed in different episodes. However, the model should be tested further by determination of the oxygen isotopic compositions of grains of dolomite and types 1 and 2 calcite in the same meteorite.

4.5. Variations in solution compositions between parent body regions

The grain-scale data acquired from each meteorite tracks the compositional evolution of aqueous solutions within discrete millimetre–centimetre size parent body regions. However, given that only small numbers of grains were analysed in each sample, these datasets cannot be used with confidence to answer the question of whether fluids evolved

differently between parent body regions. This problem of unrepresentative sampling by NanoSIMS can be addressed by using the oxygen isotopic compositions of carbonates in bulk samples of CM meteorites. Results from each sample will be an average of the meteorite's grain population, and differences between meteorite samples will indicate how grain populations vary between parent body regions.

The $\delta^{18}O$ values of carbonates in bulk samples have a wide range: ~36–20‰ (five CM chondrites analysed by Benedix et al., 2003) and ~35–15‰ (average 25‰; 45 CM chondrites analysed by Alexander et al., 2015) (Fig. 3). As the maxima and minima of these ranges are close to the compositions of types 1 and 2 calcite (i.e., ~38–32‰ and ~24–18‰, respectively; Table 4), we suggest that these two calcite types occur in many meteorites and in very different relative proportions. The latter assumption is consistent with point counting results showing that the type 1 to type 2 calcite ratio varies from 1–17, just in four CM chondrites (Table 2). The bulk meteorite data can be used to test our conclusion that $\delta^{18}O$ and $\Delta^{17}O$ fell between precipitation of the two types of calcite because meteorites with a low bulk carbonate $\delta^{18}O$ should be rich in type 2 calcite that has a relatively low $\Delta^{17}O$. Results from the five CM chondrites studied by Benedix et al. (2003), which include three of those used in the present study (Murchison, Mighei, Cold Bokkeveld), confirm that bulk carbonate $\delta^{18}O$ and $\Delta^{17}O$ covary ($r^2 = 0.62$, $n = 11$ analyses). Indeed, regression lines for NanoSIMS data acquired in the present study and the bulk data in Benedix et al. (2003) are similar (Fig. 3). To summarise, the grain-scale data from each CM chondrite shows that aqueous solutions evolved towards a lower $\delta^{18}O$ and $\Delta^{17}O$, possibly accompanied by an increase in temperature. The bulk data suggest that in some parent body regions nearly all of the calcite precipitated from cool 'juvenile' fluids giving a bulk carbonate $\delta^{18}O$ of ~35‰ (i.e., type 1). In other regions, the calcite precipitated from 'evolved' fluids that had become isotopically lighter by interaction with the parent body, and may also have been hotter. These CM chondrites are dominated by type 2 calcite and so have a bulk carbonate $\delta^{18}O$ of ~15‰. An 'average' CM chondrite will contain both calcite types and have a bulk carbonate $\delta^{18}O$ of ~25‰.

Our interpretations of the bulk carbonate data differ to those reached by Alexander et al. (2015). They concluded that fluid compositions varied little between parent body regions ($\delta^{18}O$ ~5‰) so that the ~35–15‰ range in bulk carbonate $\delta^{18}O$ values largely reflects contrasts in average temperatures (~0–130 °C). Indeed, differences in the average temperature of carbonate precipitation were demonstrated by Guo and Eiler (2007). They used clumped isotope thermometry to analyse carbonates in bulk samples of Murchison, Murray and Cold Bokkeveld. Temperatures obtained from six of seven samples were indistinguishable within error (20–35 °C, ±10 °C), but calcite in one of the three samples of Cold Bokkeveld gave a temperature of 71 °C (±10 °C). Thus there is clear evidence that fluid temperatures varied during carbonate precipitation, but our grain scale data show that solution compositions also changed. Both processes can be reconciled by envisaging one or more parent bodies within which carbonates were precipi-

tating from fluids that were increasing in temperature as they reacted with primary silicates. This temperature increase may have been linked to serpentinisation, which is an exothermic reaction.

5. IMPLICATIONS FOR MODELS OF PARENT BODY EVOLUTION

The open system model for carbonaceous chondrite aqueous alteration (Young et al., 1999) predicts that carbonates formed from aqueous solutions of a constant $\Delta^{17}O$ that had flowed along a temperature gradient would lie along a line with a slope of ~0.52 in a three-isotope plot. Results from the present study however demonstrate a coupled fall in $\delta^{18}O$ and $\Delta^{17}O$ for calcite grains within the CM chondrites (i.e., a slope of >0.52). This finding is consistent with the closed system model for aqueous alteration, which proposes that carbonates precipitated from water that was initially ^{16}O-depleted and changed in composition by reaction with ^{16}O-rich anhydrous silicates (Clayton and Mayeda, 1984, 1999). With regards to any one meteorite, the later-formed calcite grains will have a lower $\delta^{18}O$ and $\Delta^{17}O$ than those that precipitated first. Fluid temperatures probably also increased over the timespan of carbonate precipitation. Such heating need not require fluid flow and could equally have been produced locally in static solutions, for example as a by-product of serpentinisation. The very low permeability of CM carbonaceous chondrite meteorites supports the closed system model (Bland et al., 2009), as does the absence of evidence for fractionation of water-soluble elements (discussed by Velbel et al. (2012)). The presence of a vein of type 2 calcite in the CM chondrite LON 94101 (Lee et al., 2013), and dolomite veins in the CM chondrite Scott Glacier (SCO) 06043 (Lee et al., 2014), show that the late-stage 'evolved' aqueous solutions locally moved along fractures that had formed by brittle deformation of the parent body. However, given the scarcity of mineral veins in the carbonaceous chondrites in comparison to the ubiquity of type 2 calcite (Lindgren et al., 2015), it is likely that any fracture-mediated fluid flow would have been over short (~centimetre) length scales.

As the four calcite-bearing meteorites used in the present study all contain grains with a broad range of $\delta^{18}O$ values, the pattern of fluid evolution that they define must have been widespread, and such similarities in environmental conditions are underscored by the ubiquitous presence of two petrographically and isotopically distinct types of calcite. Nonetheless, the occurrence of dolomite in the most highly altered CM chondrites (CM2.0–2.2) shows that all CM chondrite parent body regions did not all evolve in exactly the same manner.

6. CONCLUSIONS

1. The broad range in oxygen isotopic compositions of calcite grains in the CM carbonaceous chondrites Murchison, Mighei, Cold Bokkeveld and LAP 031166 indicates an extended period of carbonate precipitation under changing environmental conditions;

2. The $\delta^{18}O$ and $\Delta^{17}O$ values of aqueous solutions decreased over time owing to progressive reaction with parent body silicates in a closed system, and probably in parallel with an increase in temperature. Thus, the oxygen isotopic compositions of carbonate grains in any one meteorite can be used to infer their relative order of precipitation;

3. Many CM chondrites have evidence for two discrete episodes of calcite precipitation, producing types 1 and 2 calcite, with dolomite also being formed in highly altered (i.e., CM2.0–2.2) parent body regions;

4. Grains of type 1 calcite formed by the filling of pore spaces in meteorite matrices. Calcium for these grains was sourced from dissolution of very soluble components including chondrule mesostasis, plagioclase and melilite. In any one meteorite, most type 2 calcite is interpreted to have precipitated after type 1, and by replacement of primary ferromagnesian silicate minerals;

5. Dolomite probably formed in response to a thermal pulse or a brief increase in fluid Mg/Ca. The oxygen isotopic compositions of grains in ALH 84049 and Sutter's Mill are consistent with their precipitation between types 1 and 2 calcite, but this conclusion needs to be tested by oxygen isotopic analysis of all three grain types where they occur in the same meteorite;

6. Large differences between parent body regions in the relative proportions of types 1 and 2 calcite are reflected in the wide range of isotopic compositions of carbonates in bulk meteorite samples. In some parent body regions most calcite precipitated from juvenile fluids (type 1) whereas in others it formed mainly from evolved solutions (type 2). The reasons for differences in the relative proportions of the two calcite types remain unclear, but given that type 2 calcite typically forms after type 1, it could be linked to contrasts in the longevity of aqueous alteration;

7. The ubiquitous presence within the CM carbonaceous chondrites of two petrographically and isotopically distinct generations of calcite demonstrates such a strong similarity in parent body evolution as to suggest that they could sample a single C-type asteroid.

ACKNOWLEDGEMENTS

APPENDIX A. SUPPLEMENTARY DATA

Supplementary data associated with this article can be found, in the online version, at http://dx.doi.org/10.1016/j.gca.2017.01.048.

REFERENCES

Alexander C. M. O'D., Howard K. T., Bowden R. and Fogel M. L. (2013) The classification of CM and CR chondrites using bulk H, C and N abundances and isotopic compositions. *Geochim. Cosmochim. Acta* **123**, 244–260.

Alexander C. M. O'D., Bowden R., Fogel M. L. and Howard K. T. (2015) Carbonate abundances and isotopic compositions in chondrites. *Meteorit. Planet. Sci.* **50**, 810–833.

Barber D. J. (1981) Matrix phyllosilicates and associated minerals in C2M carbonaceous chondrites. *Geochim. Cosmochim. Acta* **45**, 945–970.

Benedix G. K., Leshin L. A., Farquhar J., Jackson T. and Thiemens M. H. (2003) Carbonates in CM2 chondrites: constraints on alteration conditions from oxygen isotopic compositions and petrographic observations. *Geochim. Cosmochim. Acta* **67**, 1577–1588.

Bland P. A., Jackson M. D., Coker R. F., Cohen B. A., Webber J. B. W., Lee M. R., Duffy C. M., Chater R. J., Ardakani M. G., McPhail D. S., McComb D. W. and Benedix G. K. (2009) Why aqueous alteration in asteroids was isochemical: High porosity≠ high permeability. *Earth Planet. Sci. Lett.* **287**, 559–568.

Bonal L., Huss G. R., Krot A. N. and Nagashima K. (2010) Chondritic lithic clasts in the CB/CH-like meteorite Isheyevo: Fragments of previously unsampled parent bodies. *Geochim. Cosmochim. Acta* **74**, 2500–2522.

Brearley A. J., Saxton J. M., Lyon I. C. and Turner G. (1999) Carbonates in the Murchison CM chondrite: CL characteristics and oxygen isotopic compositions. Lunar Planet. Sci., 30, #1301.

Bunch T. E. and Chang S. (1980) Carbonaceous chondrites – II. Carbonaceous chondrite phyllosilicates and light element geochemistry as indicators of parent body processes and surface conditions. *Geochim. Cosmochim. Acta* **44**, 1543–1577.

Burbine T. H., McCoy T. J., Meibom A., Gladman B. and Keil K. (2002) Meteoritic Parent Bodies: Their Number and Identification. In *Asteroids III* (eds. , Jr.W. F. Bottke, A. Cellino, P. Paolicchi and R. P. Binzel). University of Arizona Press, pp. 653–667.

Clark B. E., Ziffer J., Nesvorny D., Campins H., Rivkin A. S., Hiroi T., Barucci M. A., Fulchignoni M., Binzel R. P., Fornasier S., DeMeo F., Ockert-Bell M. E., Licandro J. and Mothe-Diniz T. (2010) Spectroscopy of B-type asteroids: Subgroups and meteorite analogues. *J. Geophys. Res.* **115**, E06005.

Clayton R. N. and Mayeda T. K. (1984) The oxygen isotope recordin Murchison and other carbonaceous chondrites. *Earth Planet. Sci. Lett.* **67**, 151–161.

Clayton R. N. and Mayeda T. K. (1999) Oxygen isotope studies of carbonaceous chondrites. *Geochim. Cosmochim. Acta* **63**, 2089–2104.

de Leuw S., Rubin A. E., Schmidt A. K. and Wasson J. T. (2010) Carbonates in CM chondrites: Complex formational histories and comparison to carbonates in CI chondrites. *Meteorit. Planet. Sci.* **45**, 513–530.

DuFresne E. R. and Anders E. (1962) On the chemical evolution of the carbonaceous chondrites. *Geochim. Cosmochim. Acta* **26**, 1085–1114.

Emery J. P., Fernandez Y. R., Kelley M. S. P., Warden (Nee Crane) K. T., Hergenrother C., Lauretta D. S., Drake M. J., Campins H. and Ziffer J. (2014) Thermal infrared observations and thermophysical characterization of OSIRIS-REx target asteroid (101955) Bennu. *Icarus* **234**, 17–35.

Fujiya W., Sugiura N., Hotta H., Ichimura K. and Sano Y. (2012) Evidence for the late formation of hydrous asteroids from young meteoritic carbonates. *Nat. Commun.* **3**, 627.

Fujiya W., Sugira N., Marrochi Y., Takahata N., Hoppe P., Shirai K., Sano Y. and Hiyagon H. (2015) Comprehensive study of carbon and oxygen isotopic compositions, trace element abundances, and cathodoluminescence intensities of calcite in the Murchison CM chondrite. *Geochim. Cosmochim. Acta* **161**, 101–117.

Fujiya W., Fukuda K., Koike M., Ishida A. and Sano Y. (2016) Oxygen and carbon isotopic ratios of carbonates in the Nogoya CM chondrite. *Lunar Planet. Sci. 47.* Lunar Planet. Inst., Houston. #1712 (abstr.).

Guo W. and Eiler J. M. (2007) Temperatures of aqueous alteration and evidence for methane generation on the parent bodies of the CM chondrites. *Geochim. Cosmochim. Acta* **71**, 5565–5575.

Hewins R. H., Bourot-Denise M., Zanda B., Leroux H., Barrat J.-A., Humayun M., Göpel C., Greenwood R. C., Franchi I. A., Pont S., Lorand J.-P., Cournède C., Gattacceca J., Rochette P., Kuga M., Marrocchi Y. and Marty B. (2014) The Paris meteorite, the least altered CM chondrite so far. *Geochim. Cosmochim. Acta* **124**, 190–222.

Horita J. (2014) Oxygen and carbon isotope fractionation in the system dolomite–water–CO$_2$ to elevated temperatures. *Geochim. Cosmochim. Acta* **129**, 111–124.

Horstmann M., Vollmer C., Barth M.I.F., Chaussidon M., Gurenko A. and Bischoff A. (2014) Tracking aqueous alteration of CM chondrites – insights from in situ oxygen isotope measurements of calcite. *Lunar Planet. Sci.*45. Lunar Planet. Inst., Houston. #1761 (abstr.).

Howard K. T., Alexander C. M. O'D., Schrader D. L. and Dyl K. A. (2015) Classification of hydrous meteorites (CR, CM and C2 ungrouped) by phyllosilicate fraction: PSD-XRD modal mineralogy and planetesimal environments. *Geochim. Cosmochim. Acta* **149**, 206–222.

Jenniskens P., Fries M. D., Yin Q.-Z., Zolensky M., Krot A. N., Sandford S. A., Sears D., Beauford R., Ebel D. S., Friedrich J. M., Nagashima K., Wimpenny J., Yamakawa A., Nishiizumi K., Hamajima Y., Caffee M. W., Welten K. C., Laubenstein M., Davis A. M., Simon S. B., Heck P. R., Young E. D., Kohl I. E., Thiemens M. H., Nunn M. H., Mikouchi T., Hagiya K., Ohsumi K., Cahill T. A., Lawton J. A., Barnes D., Steele A., Rochette P., Verosub K. L., Gattacceca J., Cooper G., Glavin D. P., Burton A. S., Dworkin J. P., Elsila J. E., Pizzarello S., Ogliore R., Schmitt-Kopplin P., Harir M., Hertkorn N., Verchovsky A., Grady M., Nagao K., Okazaki R., Takechi H., Hiroi T., Smith K., Silber E. A., Brown P. G., Albers J., Klotz D., Hankey M., Matson R., Fries J. A., Walker R. J., Puchtel I., Lee C.-T., Erdman M. E., Eppich G. R., Roeske S., Gabelica Z., Lerche M., Nuevo M., Girten B. and Worden S. P. (2012) Radar enabled recovery of the Sutter's Mill meteorite, a carbonaceous chondrite regolith breccia. *Science* **338**, 1583–1587.

Johnson C. A. and Prinz M. (1993) Carbonate compositions in CM and CI chondrites, and implications for aqueous alteration. *Geochim. Cosmochim. Acta* **57**, 2843–2852.

Kasuga T., Usui F., Ootsubo T., Hasegawa S. and Kuroda D. (2013) High-albedo C-complex asteroids in the outer main belt: The near-infrared spectra. *Astronomical J.* **146**, 1.

Lauretta D. S., Bartels A. E., Barucci M. A., Bierhaus E. B., Binzel R. P., Bottke W. F., Campins H., Chesley S. R., Clark B. C., Clark B. E., Cloutis E. A., Connolly H. C., Crombie M. K., Delbo M., Dworkin J. P., Emery J. P., Glavin D. P., Hamilton V. E., Hergenrother C. W., Johnson C. L., Keller L. P., Michel P., Nolan M. C., Sandford S. A., Scheeres D. J., Simon A. A., Sutter B. M., Vokrouhlicky D. and Walsh K. J. (2015) The OSIRIS-REx target asteroid (101955) Bennu: Constraints on its physical, geological, and dynamical nature from astronomical observations. *Meteorit. Planet. Sci.* **50**, 834–849.

Lee M. R. (1993) The petrography, mineralogy and origins of calcium sulphate within the Cold Bokkeveld CM carbonaceous chondrite. *Meteoritics* **28**, 53–62.

Lee M. R. and Ellen R. (2008) Aragonite in the Murray (CM2) carbonaceous chondrite: Implications for parent body compaction and aqueous alteration. *Meteorit. Planet. Sci.* **43**, 1219–1231.

Lee M. R., Lindgren P., Sofe M. R., Alexander C. M. O'D. and Wang J. (2012) Extended chronologies of aqueous alteration in the CM2 carbonaceous chondrites: evidence from carbonates in Queen Alexandra Range 93005. *Geochim. Cosmochim. Acta* **92**, 148–169.

Lee M. R., Sofe M. R., Lindgren P., Starkey N. A. and Franchi I. A. (2013) The oxygen isotope evolution of parent body aqueous solutions as recorded by multiple carbonate generations in the Lonewolf Nunataks 94101 CM2 carbonaceous chondrite. *Geochim. Cosmochim. Acta* **121**, 452–466.

Lee M. R., Lindgren P. and Sofe M. R. (2014) Aragonite, breunnerite, calcite and dolomite in the CM carbonaceous chondrites: High fidelity recorders of progressive parent body aqueous alteration. *Geochim. Cosmochim. Acta* **144**, 126–156.

Lee M. R., Lindgren P., King A. J., Greenwood R. C., Franchi I. A. and Sparkes R. (2016) Elephant Moraine 96029, a very mildly aqueously altered and heated CM carbonaceous chondrite: implications for the drivers of parent body processing. *Geochim. Cosmochim. Acta* **92**, 148–169.

Lindgren P., Lee M. R., Sofe M. R. and Burchell M. J. (2011) Microstructure of calcite in the CM2 carbonaceous chondrite LON 94101: implications for deformation history during and/ or after aqueous alteration. *Earth Planet. Sci. Lett.* **306**, 289–298.

Lindgren P., Hanna R. D., Dobson K. J., Tomkinson T. and Lee M. R. (2015) The paradox between low shock-stage and evidence for compaction in CM carbonaceous chondrites explained by multiple low-intensity impacts. *Geochim. Cosmochim. Acta* **148**, 159–178.

Marrocchi Y., Gounelle M., Blanchard I., Caste F. and Kearsley A. T. (2014) The Paris meteorite: Secondary minerals and asteroidal processing. *Meteorit. Planet. Sci.* **49**, 1232–1249.

McSween H. Y. (1979a) Alteration in CM carbonaceous chondrites inferred from modal and chemical variations in matrix. *Geochim. Cosmochim. Acta* **43**, 1761–1770.

McSween, Jr., H. Y. (1979b) Are carbonaceous chondrites primitive or processed? A review. *Rev. Geophys. Space Phys.* **17**, 1059–1078.

Palguta J., Schubert G. and Travis B. J. (2010) Fluid flow and chemical alteration in carbonaceous chondrite parent bodies. *Earth Planet. Sci. Lett.* **296**, 235–243.

Rubin A. E. (2015) An American on Paris: Extent of aqueous alteration of a CM chondrite and the petrography of its refractory and amoeboid olivine inclusions. *Meteorit. Planet. Sci.* **50**, 1595–1612.

Rubin A. E., Trigo-Rodriguez J. M., Huber H. and Wasson J. T. (2007) Progressive aqueous alteration of CM carbonaceous chondrites. *Geochim. Cosmochim. Acta* **71**, 2361–2382.

Starkey N. A. and Franchi I. A. (2013) Insight into the silicate and organic reservoirs of the comet forming region. *Geochim. Cosmochim. Acta* **105**, 73–91.

Tomeoka K. and Buseck P. R. (1985) Indicators of aqueous alteration in CM carbonaceous chondrites: microtextures of a layered mineral containing Fe, S, O, and Ni. *Geochim. Cosmochim. Acta* **49**, 2149–2163.

Tyra M. A., Farquhar J., Wing B. A., Benedix G. K., Jull A. J. T., Jackson T. and Thiemens M. H. (2007) Terrestrial alteration of carbonate in a suite of Antarctic CM chondrites: Evidence from

oxygen and carbon isotopes. *Geochim. Cosmochim. Acta* **71**, 782–795.

Tyra M. A., Farquhar J., Guan Y. and Leshin L. A. (2012) An oxygen isotope dichotomy in CM2 chondritic carbonates – a SIMS approach. *Geochim. Cosmochim. Acta* **77**, 383–395.

Tyra M. A., Brearley A. and Guan Y. (2016) Episodic carbonate precipitation in the CM chondrite ALH 84049: An ion microprobe analysis of O and C isotopes. *Geochim. Cosmochim. Acta* **175**, 195–207.

Velbel M. A., Tonui E. K. and Zolensky M. E. (2012) Replacement of olivine by serpentine in the carbonaceous chondrite Nogoya (CM2). *Geochim. Cosmochim. Acta* **87**, 117–135.

Young E. D. (2001) The hydrology of carbonaceous chondrite parent bodies and the evolution of planet progenitors. *Philos. Trans. R. Soc. London, Ser. A* **359**, 2095–2110.

Young E. D., Ash R. D., England P. and Rumble, III, D. (1999) Fluid flow in chondritic parent bodies: Deciphering the compositions of planetesimals. *Science* **286**, 1331–1335.

Associate editor: Alexander Krot